Calcium Impregnation in Mesoporous Silica Made using Methyl Ricinoleate as Template and Its Application as Transesterification Catalyst

Andriayani[1,2*], Marpongahtun[1,5], Yugia Muis[1], Dikki Novran[3] and Justaman Karokaro[4]
[1]*Chemistry Department, Universitas Sumatera Utara, Jl. Bioteknologi No 1, Medan, Indonesia*
[2]*Pusat Kajian IPTEK Minyak Atsiri Euca plytu, Universitas Sumatera Utara, Jl. Bioteknologi No 1, Medan, Indonesia*
[3]*Degree Program Chemistry Department, Universitas Sumatera Utara, Jl. Bioteknologi No 1, Medan, Indonesia*
[4]*Laboratorium Pengujian BARISTAM North Sumatera, Medan, Indonesia*
[5]*Laboratorium Penelitian Terpadu Universitas Sumatera Utara, Medan, Indonesia*

Keywords: Mesoporous Silica, Metil Ricinoleic, Impregnation, Calcium Oxide, Transesterification.

Abstract: The impregnation of CaO in mesoporous silica made using methyl ester ricinoleate as a template was carried out. The impregnated silica mesoporous product was applied as a catalyst in the transesterification reaction of castor oil. Silica mesoporous products before impregnation and after impregnation were characterized using FT-IR, XRD, SEM and porosity analysis using BET. Mesoporous silica data before impregnation has a significant difference compared to mesoporous silica after impregnation. Its application as a catalyst in the transesterification reaction of castor oil produces 74.44% ricin methyl ester.

1 INTRODUCTION

Porosity greatly influences the physical properties of a material such as density, heat conductivity, strength and others (Schubert, Ulrich S. and Husing, 2005). The synthesis technique of mesopore material (2-50 nm pore diameter) is currently developing rapidly because mesopore material has unique properties, such as a more regular pore structure, large surface area and uniform pore size distribution. So much applied as catalysts (Li et al., 2011), adsorbents (Yan et al., 2006), drug delivery (Slowing et al., 2008), biosensors (Hasanzadeh et al., 2012), optics (Kumari & Sahare, 2013) and others.

The synthesis technique of mesoporous material is carried out by combining inorganic components as material and organic components such as surfactants functioning as pore printers (templates). The pore will be obtained after the organic component has been removed by calcination.

In the previous study (Andriayani et al., 2013) have been done synthesized of material silica using sodium risinoleate as a template by varying the addition of HCl 0,1N. We have also examined the effect of variations in HCl concentrations in the synthesis of mesoporous silica materials using methyl ester ricinoleate as a template (Andriayani et al., 2018). In this paper, tetraethylortosilicate (TEOS) is used as a source of silica, risinolet methyl ester as a template is made by extracting Ricinus communis seeds that grow in wild forests in the North Sumatera Karo region. Also used are 3-aminopropyltrimethoxysilane (APMS) as a co-structure directing agent (CSDA). Product mesoporous silica impregnated by CaO and analyzed using FT-IR, XRD, SEM and BET. The mesoporous silica impregnation product was applied as a catalyst in the reaction of castor oil eseterification to ricinoleate ester. Given the increasingly limited fossil fuels, ricinoleic esters can be an alternative to fuels sourced from plants.

2 RESEARCH AND METHOD

2.1 Synthesis Meterial Mesopori Silika MS 8.4Me

Methyl esters of ricinoleate ($C_{19}H_{36}O_3$) 4.52 g (0.015 mol), 100 ml deionized water and 8.4 grams of methanol were put into two neck flasks and

Andriayani, ., Marpongahtun, ., Muis, Y., Novran, D. and Karokaro, J.
Calcium Impregnation in Mesoporous Silica Made using Methyl Ricinoleate as Template and Its Application as Transesterification Catalyst.
DOI: 10.5220/0010136900002775
In *Proceedings of the 1st International MIPAnet Conference on Science and Mathematics (IMC-SciMath 2019)*, pages 96-101
ISBN: 978-989-758-556-2

sterilized at room temperature for 15 minutes, and added 30 ml HCl 0.1M (mixture A). A mixture of 1.2 g (0.007 mol) APMS ($C_6H_{17}SiO_3N$) and 6.02 g (0.029 mol) TEOS ($C_8H_{20}SiO_4$) was made by stirring for 10 minutes (mixture B). The mixture (B) was added to the mixture (A) and then stirred for 2 hours. Then it is cured in an oven at 80°C for 3 days (72 hours) until a porous solid is formed. The mixture is centrifuged and the solids are separated and washed with deionized water. The solid is dried at 50°C and then calcined at 550°C for 6 hours. Silica mesoporous products were obtained as much as 1.7 g and coded MS 8.4Me. The product were characterized using FT-IR, XRD, SEM analysis and N_2 isotherm adsorption / desorption.

2.2 Impregnation Mesoporous Silica with CaO

Silica mesoporous material (MS 8.4Me-CaO) (0.36 gram) and Ca (NO3) 2 (1.18 g) were added to glass beaker and 16 grams of dried methanol were added. The mixture is stirred for 8 hours at room temperature. The mixture is vacuumed in a desiccator until the solid dries and then the solid is calcined at 650°C for 8 hours. The mesoporous silica product that has been impregnated by CaO (MS 8,4Me-CaO) is characterization using FT-IR, XRD, AAS, BET and SEM.

2.3 Application of Mesoporous silica-CaO (MS 8.4Me-CaO) as a Catalyst in Transesterification of Castor Oil

Mesoporous silica-CaO (MS 8.4Me-CaO) (0.2 gram), methanol (p.a) (6.14 gram) and castor oil (15 gram) were put into a two neck flask. The mixture is stirred with a magnetic stirrer for 4 hours at a temperature of 80°C by the reflux method. After the reaction is complete the silica-CaO mesoporous solid is separated by filtration. The filtrate was extracted using n-hexane and distilled water. The n-hexane phase was vacuum and a pale yellow methyl ester product was obtained 9.21 grams (61.4%). The methyl ester product was characterized using FT-IR and GC-MS.

3 RESULT AND DISCUSSION

3.1 Characteristics of Mesoporous Silica (MS 8.4Me) before and after CaO Impregnation

Synthesis of mesoporous silica was carried out using methyl ester ricinoleate as a template, tetraethylortosilicate as a source of silica, the addition of 8.4 grams of methanol and the maturation process in an oven at 80 C for 72 hours. The solids were separated by centrifugation, washed, dried and calcined at 550C for 6 hours and obtained 1.6 grams of mesoporous silica (MS 8.4Me) white solids (figure 1A) Then the silica mesoporous product was pregnated with CaO and calcined at 650 padaC for 8 hours and white silica-CaO mesoporous solids (MS 8.4Me-CaO) were obtained 0.47 grams (Figure 1B).

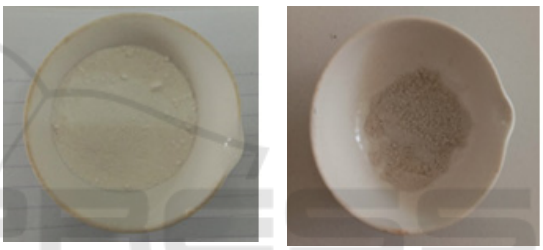

A B

Figure 1: Product of mesopori silica (MS 8.4Me): (A) before and (B) after CaO impregnation.

Changes that occur in the silica mesoporous function groups before impregnation and after CaO impregnation can be proven using FT-IR spectrum based on wave number data. Spectrum Ft-IR of mesoporous silica prior to impregnation (MS 8.4Me) (Figure 2 black) showed an absorption peak at 3421.72 cm^{-1} widening due to the presence of OH (Si-OH) strain on the surface of silica material. This is also supported by the absorption peak at 952.84 cm^{-1} due to strain (–SiO-H). The absorption peak at 1103.28 cm^{-1} is sharp due to the asymmetric streaching of Si-O-Si (υas Si-O-Si) and the wave number at 806.25 cm^{-1} due to symmetric streaching of Si-O-Si (υs Si-O- Si). Spectrum data adjusted for literature: (AlOthman & Apblett, 2010; Khalil, 2007; Liu et al., 2010; Zhao et al., 2011). FT-IR spectra of mesoporous silica after impregnation of CaO (MS 8,4Me-CaO) (Figure 2 in red). The peak absorption at 3425.58 cm^{-1} is widened due to the OH

group strain (Si-OH). Another absorption peak is seen at 1099.43 cm^{-1} which is strong due to the asymmetric strain of Si-O-Si (υas Si-O-Si) and supported symmetric streching of Si-O-Si (υs Si-O-Si) at 513.07 cm^{-1}. Changes in the function of mesoporous silica impregnation of CaO (MS 8,4Me-CaO) (Figure 2 in red) show the absorption peak at 956.69 cm^{-1} which is widening and appears to overlap with Si-O-Si asymmetrical absorption at 1099.43 cm^{-1}. This is due to the existence of the Si-O-Ca- group. This is due to the mesoporous that has been impregnated by the formation of Si-O-M bonds (M = metal) which is in the wave number 1000-900 with a strong band (Smith, 1960). This proves that the surface of mesoporous silica has been impregnated by CaO and is supported by the low intensity of absorption of the -Si-OH group in MS 8.4Me-CaO (68.67 a.u) compared to MS 8.4Me before impregnation (78.78 au).

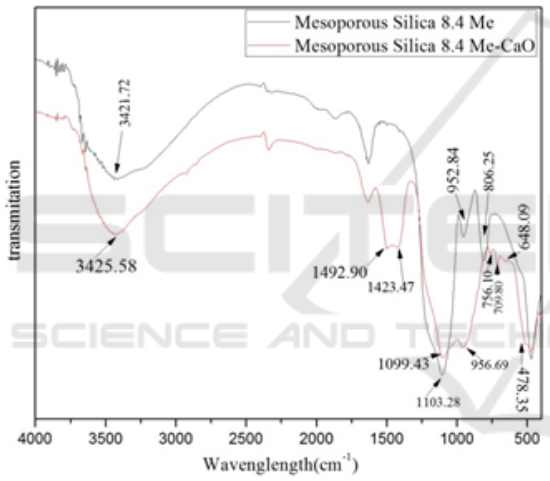

Figure 2: Spectrum FT-IR mesopori silica before impregnation (MS 8.4Me) and after CaO impregnation (MS 8.4Me-CaO).

Analysis of the structure of mesoporous silica material before impregnation and after impregnation of CaO (Figure 3) shows diffraction of X-ray diffraction (XRD). The mesoporous silica diffractogram before impregnation (MS 8.4Me) (Figure 3 in black) at an angle of 2 theses shows the diffractogram shape broad (broad) with the peak of the diffractogram at 24.0°, this shows that the silica mesopore material is nanoparticles and is amorphous. This is consistent with data reported by previous researchers (Li et al. 2011; Zhao et al. 2011; Shah, Li, and Ali Abdalla 2009; Khalil 2007; and Park et al. 2006). XRD diffractogram mesoporous silica impregnation of CaO (MS 8.4 Me-CaO) (Figure 3 in red) shows the change in the shape of the diffractogram. XRD diffractogram mesoporous silica impregnation of CaO (MS 8.4 Me-CaO) (Figure 3 in red) shows a change in the shape of the diffractogram. Si atom diffractogram shifts at 24°, whereas the diffractogram peaks at 32°, 41°, 46° indicate the presence of impregnated Ca metal on the silica surface. This is in accordance with the references of Albuquerque et al. (2008).

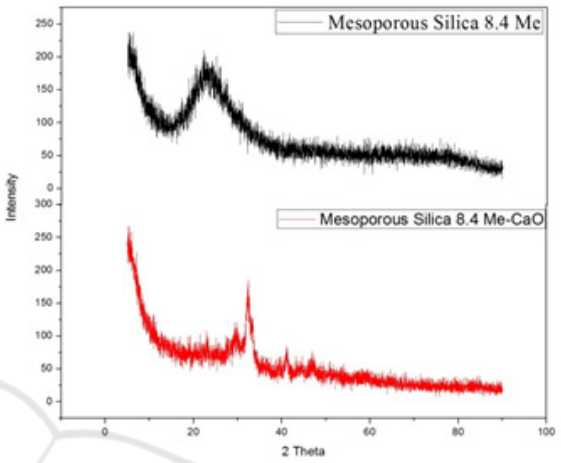

Figure 3: Diffractogram XRD of mesoporous silica before and after CaO impregnation.

Analysis of silica material porosity before impregnation and after impregnation of CaO (Figure 4) shows that there are differences in the adsorption/desorption isotherm graphs. Graph adsorption/desoprtion isotherm of mesoporous silica before impregnation (Figure 4 in black) based on the shape of the lop hysteresis is approaching Type IV according to the specific IUPAC classification for silica mesoporous material. The shape of lop hysteresis is Type H3 and Type H4, where the shape of lop hysteresis is a bit more complex because the reversible micropore filling area is followed by multilayer physisorption and capillary condensation, so that Lop H4 is the same as Lop H3 for non-micropore material. This is adjusted by reference (Sing & Williams, 2004). While the adsorption graph desorption of isotherm of silica mesoporous material after impregnation Figure 4 in red) lop hysteresis form is Type H3 according to Sing and Williams (2004) reference, this is due to aggregate and plate particle shape, characteristic desorption indentation and lower approaching end point (Lop). closure point). Lop H3 does not have a plateau at high P/P0 values (mesoporous volume is not well formulated), so interpretation of high P/P0 values is more difficult. Branch adsorption graphs on type H3 show that gas adsorption only occurs on surfaces or

manolayers so that this shows that the obtained silica material can be grouped also on Type II isotherm charts for non-porous solids (Gregg S. J., and Sing, 1982). This is due to the silica impregnated surface of CaO in the pores that are already covered by CaO so that the shape of the hysteresis lop resembles non-pore solids.

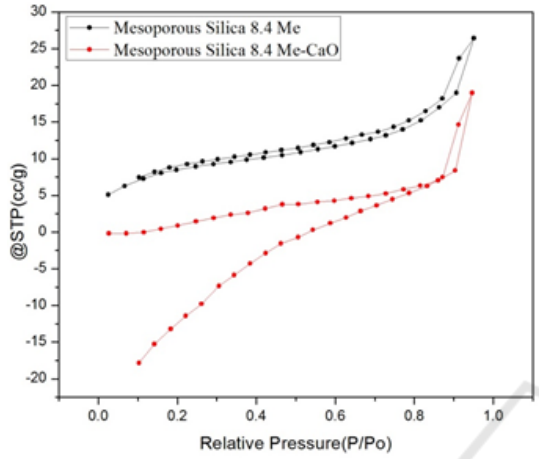

Figure 4: Graph adsorption/desorption isotherm of mesopore silica before and after CaO impregnation.

The graph of pore size distribution mesoporous silica before and after the pre-impregnation of CaO calculated using the Barret-Joyner-Halenda (BJH) method can be seen in (Figure 5). The mesopore pore size distribution before impregnation (Figure 5 in black) shows the pore size distribution in the range 1.59 nm - 9.4 nm. While the pore size distribution of silica mesoporous material after CaO impregnation (Figure 5 in red) shows the pore size distribution in the range of 1.63 nm - 6.63 nm. The pore size distribution graph of the two materials has a difference in the value of dV/dD, which is because the calcination treatment again after the impregnation of CaO causes the dV/dD value to be lower, because the pore is already covered by the metal Ca. While silica mesoporous material before impregnation the dV/dD value is greater in the same pore size distribution range because the pores are not covered by metal.

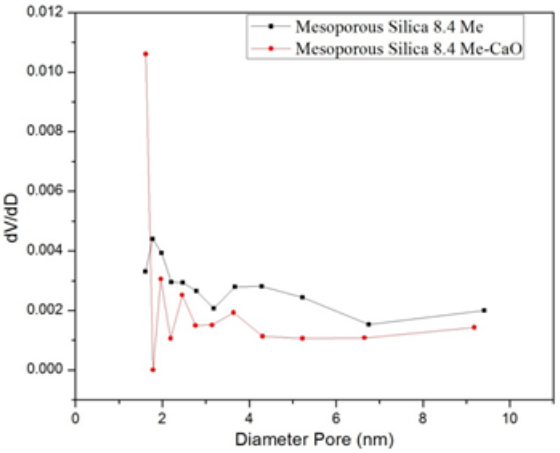

Figure 5: Graph adsorption/desorption isotherm of mesopore silica before and after CaO impregnation.

3.2 Catalytic Activity of Mesoporous Silica (MS 8,4Me-CaO)

The mesoporous silica impregnation CaO (MS 8.4Me CaO) was tested for its catalytic activity in the transesterification reaction of castor oil. The catalytic system of esterification reactions takes place under heterogeneous conditions where the silica-CaO mesoporous is insoluble (remains in a solid state). This reaction condition is advantageous because it is easily separated between the product and the catalyst. The reaction was carried out at 80°C for 4 hours. After the reaction was stopped, the catalyst solids were separated and the filtrate was extracted with n-hexane and washed with distilled water, after which it was obtained a pale yellow methyl ester product of 9.21 grams (70.6%) (Figure 6). The ricinoleate methyl ester product was characterized using FT-IR and GC-MS.

Figure 6: Product methyl esters of transesterification castor oil catalized by mesoporous silica CaO impregnation (MS 8.4Me CaO).

Proving the formation of ricinoleic methyl esters from transesterification of castor oil catalysts catalyzed by silica mesreori impregnation of CaO (MS 8.4Me-CaO), the functional group changes were analyzed using FT-IR instruments and compared with the FT-IR spectrum of castor oil

before transesterification (Figure 7). The FT-IR spectrum of methyl ester (Figure 7 in red) shows a widening peak at 3417.86 cm^{-1} due to the stretching vibrations of the OH group, while sharp peaks at 2924.09 cm^{-1} and 2854.65 cm^{-1} due to vibrational frequencies stretching -CH- (sp^3) alkane from the hydrocarbon chain. The sharp peak at 1743.65 cm^{-1} is due to the stretching vibration of C = O carbonyl methyl ester ricinoleate and is supported by the peak vibration buckling C-O at 1242.16 and 1165 cm^{-1}. The peak at 3417.86 cm^{-1} is due to the presence of OH groups from methyl ricinoleate on the C-12 atom. Compared to the FT-IR spectrum of castor oil before transesterification (Figure 7 in black) shows the low absorption intensity of C-O and C = O stretching vibrations, this shows the formation of methyl esters from castor oil.

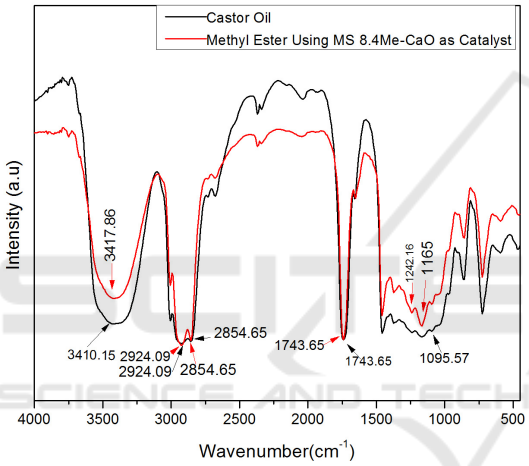

Figure 7: Spectrum FT-IR of castor oil and methyl esters from transesterification castor oil by mesoporous silica impregnation CaO (MS 8.4Me-CaO).

Transeterification of castor oil using MS 8.4 Me-CaO mesoporous silica catalysts produced a mixture of methyl esters of fatty acids. This is due to the extracted castor oil from castor bean seeds (Ricinus communis) containing several fatty acids such as: ricinoleic acid (87.7-90.4%), linoleic acid (4.1-4.7%), oleic acid (2.2-3.3%), stearic acid (0.7-1.1%), linolenic acid (0.5-0.7%) (Setiadji et al., 2017). So that if esterified other fatty acids might also be esterified. To find out the composition of methyl esters formed from castor oil, GC-MS analysis was performed. GC-MS data results showed that the percentage of methyl ester ricinoleate was 74.44%. While the remaining 25.56% is esters of other fatty acids. According to the literature, the composition of ricinoleic acid is around 87.7-90.4% so it can be assumed that the total methyl ester formed reaches 84.88%. The results showed that only a small portion of ricinoleic acid was not converted to its methyl ester. This is because the reaction is reversible and is influenced by several factors such as: ratio (methanol: oil: catalyst), reaction time and temperature.

Table 1 shows the results of the MS 8.4Me-CaO-catalyzed transesterification reaction, the highest yield was methyl ester ricinoleate. The transesterification reaction of castor oil using different catalysts results in different components and the amount of methyl ester formed.

Table 1: GC-MS analysis of the composition methyl esters of castor oil esterification with mesoporous silica 8.4Me-CaO catalyst.

No	Methyl ester	Molecular Formula	Molecular Weight (g/mol)	Area %
1	Methyl stearate	$C_{19}H_{38}O_2$	298	1.19
2	9,12-Octadecadienoic acid, metyl ester	$C_{19}H_{34}O_2$	294	2.95
3	Methyil 11-octadecenoate	$C_{19}H_{36}O_2$	296	3.30
4	Methyil caprate	$C_{11}H_{22}O_2$	186	1.13
5	Methyl ricinoleate	$C_{19}H_{36}O_3$	312	74.44
6	13-Heptadecyn-1-ol	$C_{17}H_{32}O$	252	16.99

4 CONCLUSIONS

The impregnation of CaO in mesoporous silica prepared using methyl ester ricinoleic as a template was carried out and the product obtained was applied as a catalyst in the castor oil transesterification reaction. Mesoporous silica impregnation product (MS 8.4Me-CaO) was characterized using FT-IR, XRD, SEM and porosity analysis using BET. The data obtained have a significant difference compared to mesoporous silica (MS 8.4Me) before being impregnated. Its application as a catalyst in the transesterification reaction of castor oil produces 74.44% methyl ester ricinoleic acid.

ACKNOWLEDGEMENTS

The authors are grateful for the main financial support from Ministry of Research, Technology and Higher Education, Republic of Indonesia through the Decentalization- Penelitian Unggulan Perguruan Tinggi (PTUPT) Research Grant 2019, coordinated by Directorate of Research and Community Services, Universitas Sumatera Utara (DRPM-USU) with Contract No: 138/UN5.2.3.1/PPM/KP-DRPM/2019.

REFERENCES

Albuquerque, M. C. G., Jiménez-Urbistondo, I., Santamaría-González, J., Mérida-Robles, J. M., Moreno-Tost, R., Rodríguez-Castellón, E., Jiménez-López, A., Azevedo, D. C. S., Cavalcante Jr., C. L., & Maireles-Torres, P. (2008). CaO supported on mesoporous silicas as basic catalysts for transesterification reactions. *Applied Catalysis A: General*, *334*(1–2), 35–43. https://doi.org/ https://doi.org/10.1016/j.apcata.2007.09.028

AlOthman, Z. A., & Apblett, A. W. (2010). Synthesis and characterization of a hexagonal mesoporous silica with enhanced thermal and hydrothermal stabilities. *Applied Surface Science*, *256*(11), 3573–3580. https://doi.org/10.1016/j.apsusc.2009.12.157

Andriayani, A., Sembiring, S. B., Aksara, N., & Sofyan, N. (2013). Synthesis of Mesoporous Silica from Tetraethylorthosilicate by Using Sodium Ricinoleic as a Template and 3-Aminopropyltrimethoxysilane as Co-Structure Directing Agent with Volume Variation of Hydrochloric Acid 0.1 M. *Advanced Materials Research*, *789*, 124–131. https://doi.org/10.4028/ www.scientific.net/AMR.789.124

Andriayani, Nainggolan, H., Taufik, M., Simamora, S., & Sofyan, N. (2018). The effect concentration of tetraethylorthosilicate and variation HCl 0.1M for synthesis mesoporous silica using oleic acid as template and 3-aminopropyltrimethoxysilane as co-structure directing Agent. *Journal of Physics: Conference Series*, *1116*(4), 0–8. https://doi.org/10.1088/1742-6596/1116/4/042006

Gregg S. J., and Sing, K. S. W. (1982). *Adsorpsi, Surface Area and Porosity* (Second Edi). Academic Press.

Hasanzadeh, M., Shadjou, N., de la Guardia, M., Eskandani, M., & Sheikhzadeh, P. (2012). Mesoporous silica-based materials for use in biosensors. *TrAC - Trends in Analytical Chemistry*, *33*, 117–129. https://doi.org/10.1016/j.trac.2011.10.011

Khalil, K. M. S. (2007). Cerium modified MCM-41 nanocomposite materials via a nonhydrothermal direct method at room temperature. *Journal of Colloid and Interface Science*, *315*(2), 562–568. https://doi.org/10.1016/j.jcis.2007.07.030

Kumari, S., & Sahare, P. D. (2013). Optical studies of fluorescent mesoporous silica nanoparticles. *Journal of Materials Science and Technology*, *29*(8), 742–746. https://doi.org/10.1016/j.jmst.2013.05.013

Li, B., Ma, W., Han, C., Liu, J., Pang, X., & Gao, X. (2011). Preparation of MCM-41 incorporated with transition metal substituted polyoxometalate and its catalytic performance in esterification. *Microporous and Mesoporous Materials*, *156*(1), 73–79. https://doi.org/10.1016/j.micromeso.2012.02.017

Liu, H., Lu, G., Guo, Y., Wang, Y., & Guo, Y. (2010). Synthesis of spherical-like Pt-MCM-41 meso-materials with high catalytic performance for hydrogenation of nitrobenzene. *Journal of Colloid and Interface Science*, *346*(2), 486–493. https://doi.org/10.1016/j.jcis.2010.03.018

Park, Y., Kang, T., Kim, P., & Yi, J. (2006). Encapsulation method for the dispersion of NiO onto ordered mesoporous silica, SBA-15, using polyethylene oxide (PEO). *Journal of Colloid and Interface Science*, *295*(2), 464–471. https://doi.org/10.1016/j.jcis.2005.09.006

Schubert, Ulrich S. and Husing, N. (2005). *Synthesis of Inorganic Materials* (2nd, Revis ed.). Wiley-VCH.

Setiadji, S., B, N. T., Sudiarti, T., H, E. P., & N, B. W. (2017). *Alternatif Pembuatan Biodiesel Melalui Transesterifikasi Minyak Castor (Ricinus communis) Menggunakan Katalis Campuran Cangkang Telur Ayam dan Kaolin*. *3*(1), 1–10.

Shah, A. T., Li, B., & Ali Abdalla, Z. E. (2009). Direct synthesis of Ti-containing SBA-16-type mesoporous material by the evaporation-induced self-assembly method and its catalytic performance for oxidative desulfurization. *Journal of Colloid and Interface Science*, *336*(2), 707–711. https://doi.org/10.1016/j.jcis.2009.04.026

Sing, K. S. W., & Williams, R. T. (2004). *Physisorption Hysteresis Loops and the Characterization of Nanoporous Materials*. *1*, 773–782. https://doi.org/10.1260/0263617053499032

Slowing, I. I., Vivero-Escoto, J. L., Wu, C. W., & Lin, V. S. Y. (2008). Mesoporous silica nanoparticles as controlled release drug delivery and gene transfection carriers. *Advanced Drug Delivery Reviews*, *60*(11), 1278–1288. https://doi.org/10.1016/j.addr.2008.03.012

Smith, A. L. (1960). Infrared spectra-structure correlations for organosilicon compounds. *Spectrochimica Acta*, *16*(1–2), 87–105. https://doi.org/10.1016/0371-1951(60)80074-4

Yan, Z., Li, G., Mu, L., & Tao, S. (2006). Pyridine-functionalized mesoporous silica as an efficient adsorbent for the removal of acid dyestuffs. *Journal of Materials Chemistry*, *16*(18), 1717–1725. https://doi.org/10.1039/b517017f

Zhao, Q., Zhou, X., Ji, M., Ding, H., Jiang, T., Li, C., & Yin, H. (2011). Stability and textural properties of cobalt incorporated MCM-48 mesoporous molecular sieve. *Applied Surface Science*, *257*(7), 2436–2442. https://doi.org/10.1016/j.apsusc.2010.09.114